

# Robust Real-Time Control of a Two-Rotor Aerodynamic System

Petko H. Petkov\* Nicolai D. Christov\*\*  
Mihail M. Konstantinov\*\*\*

\* Technical University of Sofia, 1000 Sofia, Bulgaria  
(e-mail: php@tu-sofia.bg)

\*\* Université des Sciences et Technologies de Lille, 59655 Villeneuve  
d'Ascq, France (e-mail: Nicolai.Christov@univ-lille1.fr)

\*\*\* University of Architecture, Civil Engineering and Geodesy, 1046  
Sofia, Bulgaria (e-mail: mmk\_fte@uacg.bg)

**Abstract:** This paper presents the design and experimental evaluation of a two-degree-of-freedom discrete-time  $\mu$ -controller for a laboratory two-rotor aerodynamic system with ten uncertain parameters. The controller implemented is of 24th order and ensures robust stability and robust performance of the closed-loop sampled-data system. This controller is realized on a PC by using the Real Time Workshop of MATLAB® with a sampling frequency of 100 Hz. The experimental results are close to the results predicted by using the linearized model of the system and highlight many of the difficulties associated with the practical implementation of robust control laws.

**Keywords:** Robust control; aerodynamic system;  $\mu$ -synthesis; real-time control.

## 1. INTRODUCTION

The real implementation of robust control laws is useful in teaching the modern Robust Control Theory. Such implementation allows to attract the students attention to the theoretical and practical difficulties associated with the realization of high-order controllers in presence of uncertainties, nonlinearities, disturbances and noises. The combined usage of theoretical methods, software for computer-aided design and sophisticated laboratory equipment helps to build the necessary knowledge and engineering abilities for control of complex systems.

This paper presents the design and experimental evaluation of a two-degree-of-freedom discrete-time  $\mu$ -controller for a laboratory two-rotor aerodynamic system with ten uncertain parameters. The controller implemented is of 24th order and ensures robust stability and robust performance of the closed-loop sampled-data system. This controller is realized on a PC by using the Real Time Workshop of MATLAB® with sampling frequency of 100 Hz. The experimental results are close to the results predicted by using the linearized model of the system and highlight some of the difficulties associated with the implementation of robust control laws. The controller design and implementation are used in the laboratory exercises in a course on Robust and Optimal Control, taught in the Technical University of Sofia.

## 2. SYSTEM DESCRIPTION

The two-rotor aerodynamic system (TRAS) is shown in Figure 1. There are two propellers at the both ends of a beam, driven by DC motors, joined to the base with an articulation. The main propeller controls the beam



Fig. 1. Two-rotor aerodynamic system

position in the vertical plane, while the tail propeller controls the beam position in the horizontal plane. There are two counter-weights fixed to the beam that determine the stable equilibrium position. The system is balanced in such a way, that when the motors are switched off, the main rotor end of beam is lowered. The control actions are the motor supply voltages. The measured system outputs are the two angles of beam deviation in the horizontal plane (azimuth angle) and in the vertical plane (pitch angle). The motor control is realized in pulse-width modulation (PWM) mode.

The TRAS control consists in stabilization of the beam in arbitrary (in the practical limits) desired position (pitch and azimuth) or tracking of a desired trajectory. In the design of robust control systems one usually implements

controllers obtained by  $\mathcal{H}_\infty$  design or  $\mu$ -synthesis, see Zhou et al. (1995). In this paper we present the results from  $\mu$ -synthesis only, which has the advantage that it guarantees the achievement of robust performance of the closed-loop system.

### 3. DERIVATION OF THE UNCERTAINTY MODEL

In the design of robust control laws it is advisable to use linearized models in which it is easy to set the uncertainty in specific parameters. For this aim the models, obtained by analytic linearization, are very appropriate.

In the given case the plant nonlinear model is provided by the manufacturer of the laboratory set-up in the form of nonlinear differential equations and algebraic relations as well as in the form of Simulink<sup>®</sup> model, see Anon1 (2006). The model of the two-rotor aerodynamic system is linearized analytically under the usual assumption for small deviations of the variables, describing the system behavior, around their trim values.

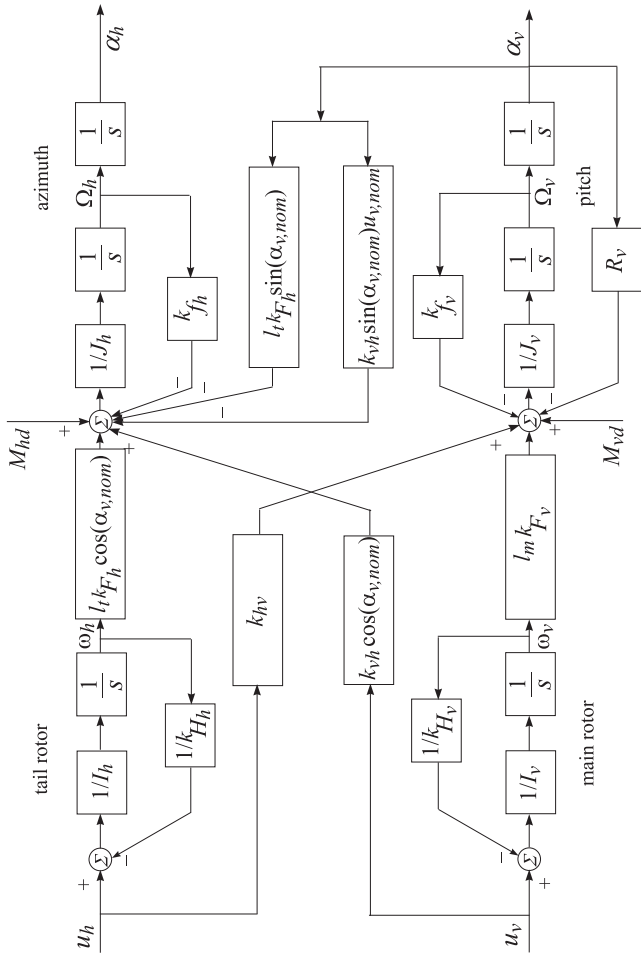


Fig. 2. Linearized model of the two-rotor aerodynamic system

The linearized TRAS model is shown in Figure 2 where the subindex *nom* denotes the nominal value of the corresponding variable. The input variables are the voltages  $u_h$  and  $u_v$  of the tail rotor and main rotor motors and output variables are the azimuth angle  $\alpha_h$  and pitch angle  $\alpha_v$ . The moments  $M_{hd}$  and  $M_{vd}$  are the disturbances acting

on the system. The plant is two-channel and there is an interaction between the two channels. In order to reveal in full the dynamic behavior of the plant it should be considered as multivariable, i.e. the two channels can not be considered as independent.

Table 1. System parameters

Symbol	Description
$I_h$	moment of inertia of the tail rotor
$J_h$	moment of inertia with respect to the vertical axis
$I_v$	moment of inertia of the main rotor
$J_v$	moment of inertia with respect to the horizontal axis
$k_{H_h}$	velocity gain of the tail rotor
$k_{F_h}$	thrust coefficient of the tail rotor
$k_{H_v}$	velocity gain of the main rotor
$k_{F_v}$	thrust coefficient of the main rotor
$k_{f_h}$	friction coefficient in the vertical axis
$k_{f_v}$	friction coefficient in the horizontal axis
$k_{h_v}$	coefficient of the cross moment from tail rotor to pitch
$k_{v_h}$	coefficient of the cross moment from main rotor to azimuth
$R_v$	coefficient of the return torque
$l_m$	length of the main part of the beam
$l_t$	length of the tail part of the beam

The parameters of the linearized model are defined in Table 1.

The coefficients  $k_{H_h}$ ,  $k_{F_h}$ ,  $k_{H_v}$ ,  $k_{F_v}$  are determined by linearization of the the corresponding rotor static characteristics, obtained experimentally. The gain  $R_v$  is the coefficient of the return torque corresponding to the forces of gravity and depends nonlinearly from the pitch angle  $\alpha_v$ . After the linearization, this gain is obtained as  $R_v = k_1 \sin(\alpha_{v,nom}) - k_2 \cos(\alpha_{v,nom})$  where  $k_1$  and  $k_2$  are constants. The inertial moment around the vertical axis,  $J_h$ , is also a nonlinear function of the pitch angle and is obtained as  $J_h = k_3 \cos^2(\alpha_{v,nom}) + k_4$ , where the coefficients  $k_3$  and  $k_4$  are determined by the mass and geometric sizes of the beam and devices mounted on it.

Table 2. Parameters of the linearized model

Parameter	Value	Units
$I_h$	1/37000	kgm <sup>2</sup>
$I_v$	1/6100	kgm <sup>2</sup>
$J_v$	$3.00581 \times 10^{-2}$	kgm <sup>2</sup>
$k_{f_h}$	$5.88996 \times 10^{-3}$	Nms/rad
$k_{f_v}$	$1.27095 \times 10^{-2}$	Nms/rad
$k_{h_v}$	$4.17495 \times 10^{-3}$	Nm
$k_{v_h}$	$-1.78200 \times 10^{-2}$	Nm
$k_{H_h}$	$9.83891 \times 10^3$	rad/s
$k_{F_h}$	$2.12932 \times 10^{-5}$	Ns/rad
$k_{H_v}$	$4.87457 \times 10^3$	rad/s
$k_{F_v}$	$3.07723 \times 10^{-4}$	Ns/rad
$l_m$	0.202	m
$l_t$	0.216	m
$k_1$	$5.00576 \times 10^{-2}$	Nm
$k_2$	$9.36008 \times 10^{-2}$	Nm
$k_3$	$2.37904 \times 10^{-2}$	kgm <sup>2</sup>
$k_4$	$3.00962 \times 10^{-3}$	kgm <sup>2</sup>

The nominal values of the model parameters are given in Table 2.

As uncertain parameters in the mathematical description of the aerodynamical system we consider the moment of inertia  $J_h$  in respect to the vertical axis, the thrust coefficients  $k_{F_h}$ ,  $k_{F_v}$  of both rotors, the velocity gains  $k_{H_h}$ ,  $k_{H_v}$  of the two rotors, the friction coefficients  $k_{f_h}$ ,  $k_{f_v}$ , the cross moment coefficients  $k_{v_h}$ ,  $k_{h_v}$ , as well as the coefficient  $R_v$  of the return torque, all together 10 parameters. The uncertainties in the moment of inertia  $J_h$  and in the coefficient  $R_v$  are due to their dependence on the pitch angle  $\alpha_v$ , the uncertainties in the coefficients  $k_{F_h}$ ,  $k_{F_v}$ ,  $k_{H_h}$ , and  $k_{H_v}$  are introduced as a result of the measuring and approximation of the static characteristics of the rotors, the uncertainties in the coefficients  $k_{f_h}$  and  $k_{f_v}$  are due to the errors in determination of the friction moments, and the uncertainties in the coefficients  $k_{v_h}$  and  $k_{h_v}$  result from simplification of the aerodynamic interaction between the two channels. Further on we assume that the moment of inertia  $J_h$  and the coefficients  $k_{F_h}$ ,  $k_{F_v}$ ,  $k_{H_h}$  and  $k_{H_v}$  are known with errors up to 10 % while the rest coefficients - with errors up to 5 %.

The ten real uncertain parameters are set by using the function `ureal` from Robust Control Toolbox, ver. 3, see Balas et al. (2006). The uncertain TRAS model is obtained on the basis of the block-diagram, shown in Figure 2, implementing the function `sysic` from the same toolbox. As a result one finds an uncertain state space object.

The uncertain TRAS system is described as a control plant by the equation

$$y = G \begin{bmatrix} M_d \\ u \end{bmatrix},$$

where

$$y = \begin{bmatrix} \alpha_h \\ \alpha_v \end{bmatrix}, u = \begin{bmatrix} u_h \\ u_v \end{bmatrix}, M_d = \begin{bmatrix} M_{hd} \\ M_{vd} \end{bmatrix}.$$

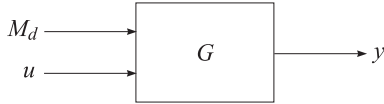


Fig. 3. Uncertain model of the TRAS system

The uncertain model of the two-rotor aerodynamic system is shown in Figure 3.

Let us introduce the representation

$$G = [G_d \ G_u]$$

such that

$$y = G_d M_d + G_u u.$$

In the last expression  $G_d$  is the plant transfer function in respect to disturbances and  $G_u$  is the plant transfer function with respect to control.

The frequency response plot of the uncertain plant singular values, obtained from the transfer function  $G_u$ , is shown in Figure 4.

#### 4. $\mu$ -SYNTHESIS OF A DISCRETE-TIME CONTROLLER

The block-diagram of the closed-loop system that includes the uncertain TRAS model, the feedback and the controller, as well as the elements reflecting the performance requirements, is shown in Figure 5.

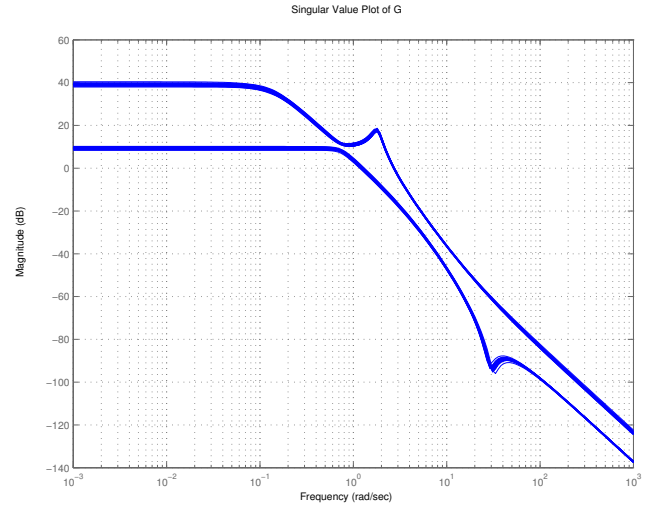


Fig. 4. Frequency response characteristics of the uncertain plant

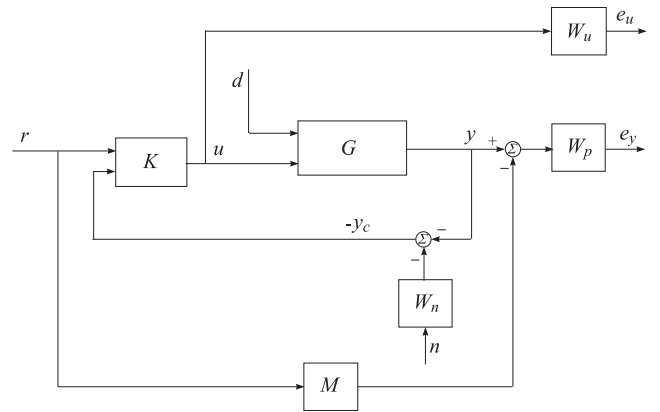


Fig. 5. Block-diagram of the closed-loop system with performance requirements

The system has reference inputs ( $r$ ), input disturbances ( $d$ ) and noise ( $n$ ) introduced in measurement of the angles  $\alpha_h$  and  $\alpha_v$ . (Here and further on the disturbance vector is denoted for brevity by  $d$ .) The TRAS uncertain model is the state space object  $G$ .

The system has two output signals ( $e_y$  and  $e_u$ ). The block  $M$  is the ideal dynamics model that the designed closed-loop system should match to. The feedback of the system is realized by the vector  $y_c = y + W_n n$ , where the measurement noise  $n$  is a random vector with unit 2-norm and  $W_n$  is the transfer matrix of the noise shaping filters.

The transfer function matrix  $M$  of the ideal matching model is chosen as diagonal in order to suppress the interaction between the two channels and is taken as

$$M(s) = \begin{bmatrix} w_{m1} & 0 \\ 0 & w_{m2} \end{bmatrix}$$

where

$$w_{m1} = \frac{1}{1.5s^2 + 1.2s + 1},$$

$$w_{m2} = \frac{1}{2.0s^2 + 1.6s + 1}.$$

In the choice of this model it was assumed that the azimuth dynamics is faster than the pitch dynamics.

The noise transfer function matrix is taken as

$$W_n(s) = \begin{bmatrix} w_n & 0 \\ 0 & w_n \end{bmatrix}$$

where  $w_n = 10^{-2} \frac{s}{s+1}$  is a high pass filter whose output is significant above 10 rad/s.

To obtain good performance of the system responses we shall implement a two-degree-of-freedom controller, see Gu et al. (2005). The control actions are generated according to the expression

$$u = [K_r \ K_y] \begin{bmatrix} r \\ -y_c \end{bmatrix} = K_r r - K_y y_c,$$

where  $K_y$  is the output feedback transfer function matrix and  $K_r$  is the pre-filter transfer function matrix.

The control actions are realized by a computer in real time with sampling frequency  $f_s = 100$  Hz. For this reason the  $\mu$ -synthesis is done for this sampling frequency.

Let us denote by  $P(z)$  the transfer function matrix of the discretized eighteen-input eighteen-output open-loop system, that consists of the plant model plus the weighting functions and let the block-structure  $\Delta_P$  is defined as

$$\Delta_P := \left\{ \begin{bmatrix} \Delta & 0 \\ 0 & \Delta_F \end{bmatrix} : \Delta \in \mathbb{R}^{10 \times 10}, \Delta_F \in \mathbb{C}^{6 \times 4} \right\}$$

The first block of the matrix  $\Delta_P$ , the block  $\Delta$ , corresponds to the parametric uncertainties, included in the model of the aerodynamic system. The second block  $\Delta_F$  is a fictitious uncertainty block, used to include the performance requirements into the framework of the  $\mu$ -approach. The inputs of this block are the weighted error signals  $e_y$  and  $e_u$ , and the outputs are the exogenous signals  $r$ ,  $d$  and  $n$ .

The aim of the  $\mu$ -synthesis is to find a stabilizing controller  $K$ , such that for each frequency  $\omega \in [0, \pi/T_s]$ , where  $T_s = 2\pi/f_s$ , the structured singular value  $\mu$  satisfies the condition

$$\mu_{\Delta_P}[F_L(P, K)(j\omega)] < 1,$$

where  $F_L(P, K)$  is the closed-loop transfer function matrix. The fulfilment of this condition guarantees the robust performance of the closed-loop system, i.e.

$$\left\| \begin{bmatrix} W_p(S_o G_u K_r - M) & W_p S_o G_d & -W_p S_o G_u K_y W_n \\ W_u S_i K_r & -W_u S_i K_y G_d & -W_u S_i K_y W_n \end{bmatrix} \right\|_{\infty} < 1$$

for all uncertainties  $\Delta$  with  $\|\Delta\|_{\infty} < 1$ , where  $S_i$  and  $S_o$  are the input and output sensitivity functions, respectively.

The  $\mu$ -synthesis is done for several performance weighting functions that ensure a good balance between system performance and robustness. On the basis of the experimental results, we choose the performance weighting function

$$W_p(s) = \begin{bmatrix} 8.4 \times 10^{-2} \frac{80s+1}{80s+10^{-3}} & -0.01 \\ 0.03 & 7.5 \times 10^{-1} \frac{500s+1}{500s+10^{-3}} \end{bmatrix}$$

and the control weighting function

$$W_u(s) = \begin{bmatrix} 4.8 \times 10^{-5} \frac{0.05s+1}{10^{-4}s+1} & 0 \\ 0 & 2.304 \times 10^{-4} \frac{0.1s+1}{10^{-4}s+1} \end{bmatrix}.$$

The frequency responses of the inverse performance and control weighting functions are given in Figures 6 and 7,

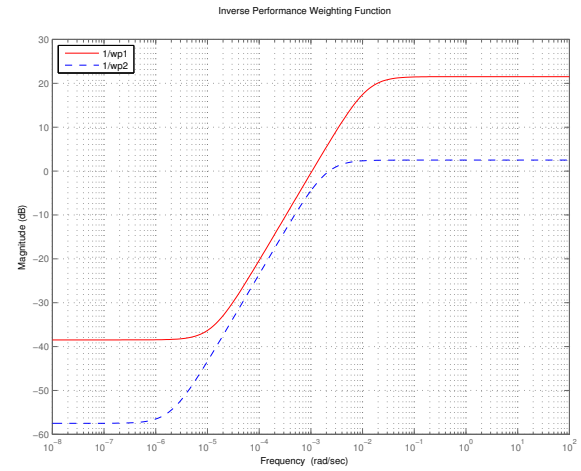


Fig. 6. Inverse performance weighting functions

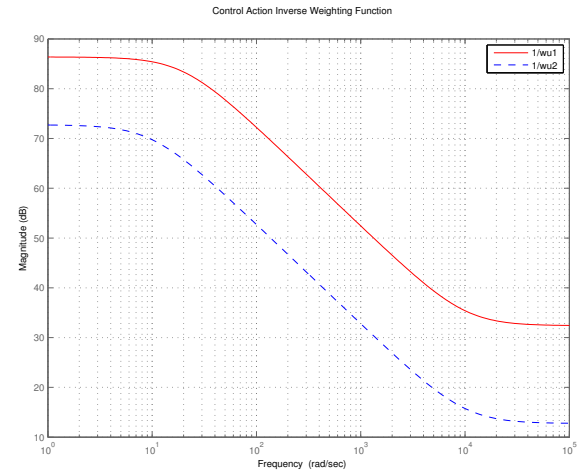


Fig. 7. Inverse control action weighting functions

respectively. The control weighting functions are chosen as high pass filters with appropriate bandwidth in order to impose constraints on the spectrum of the control actions.

The experiments with the control laws designed shows that the behavior of the real closed-loop system is very sensitive to the weighting functions used. That is why the precise tuning of the weighting functions requires a large volume of experiments.

The  $\mu$ -synthesis is performed by using the function `dksyn` from Robust Control Toolbox. Five iterations are performed that decrease the maximum value of  $\mu$  to 0.997. The final controller obtained is of 24th order. At first glance, the order of this controller is very high, which eventually makes difficult its real time implementation. In fact, the experiments show that with the relatively low sampling frequency and fast processor, the implementation of this controller does not create difficulties. That is why controller order reduction is not necessary.

The frequency response of  $\mu$ , corresponding to the robust performance analysis, is shown in Figure 8. Obviously, the closed-loop system achieves robust performance, which also guarantees robust stability of this system.

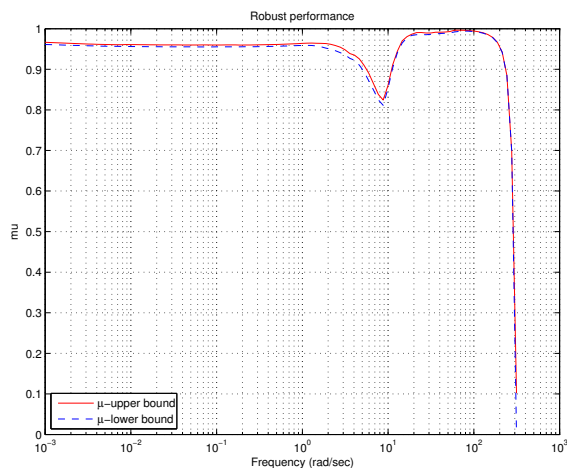


Fig. 8. Closed-loop system robust performance

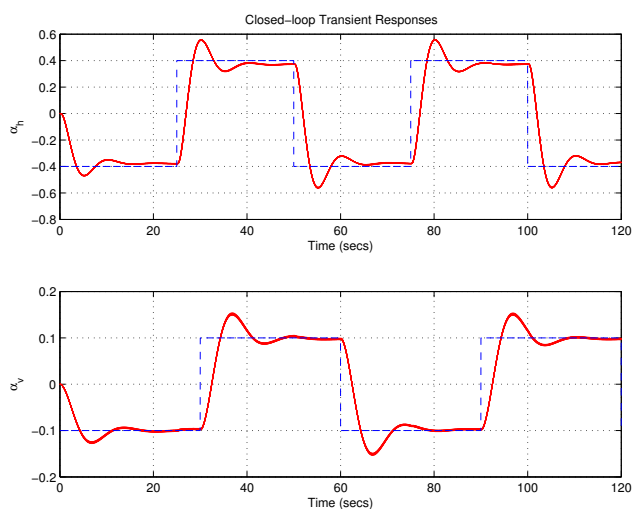


Fig. 9. Transient responses of the uncertain linear closed-loop system

The transient responses of the sampled-data closed-loop system, obtained for different random values of the uncertain parameters, are shown in Figure 9.

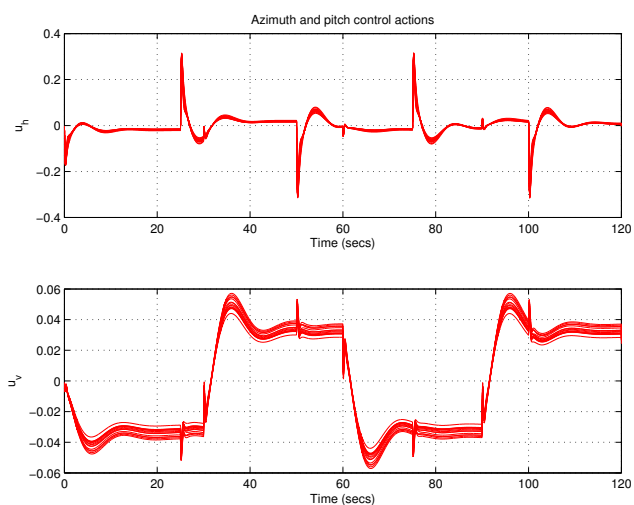


Fig. 10. Control actions of the uncertain linear closed-loop system

The control actions for different values of the uncertain parameters are shown in Figure 10.

The experiments with the controller designed show a strong influence of the control action constraints (the actuators saturation) on the performance of the closed-loop system. In some cases the usage of weighting functions ensuring very good transient responses of the linear closed-loop system leads to generation of auto-oscillations in the real system and loss of stability. A very serious influence on the dynamics of the closed-loop system may have the noises at the actuator inputs, whose level is very high in the case under consideration. This justifies the inclusion of the noises in the controller design.

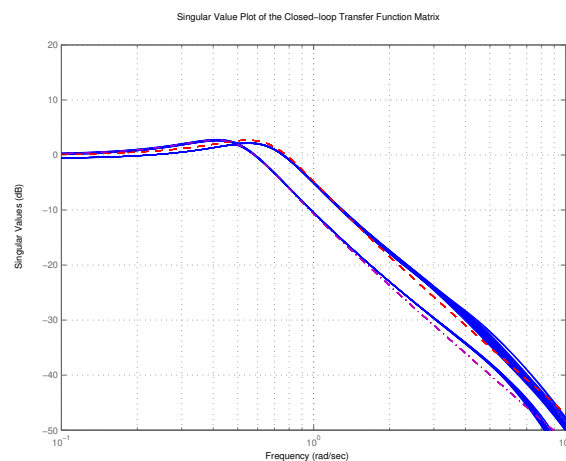


Fig. 11. Singular value plot of the closed-loop system

The frequency responses of the singular values of the closed-loop transfer function matrix for random values of the plant uncertain parameters are shown in Figure 11. It is seen that as a result of achieving robust performance, the closed-loop system frequency responses are close to these of the model (shown with dashed lines).

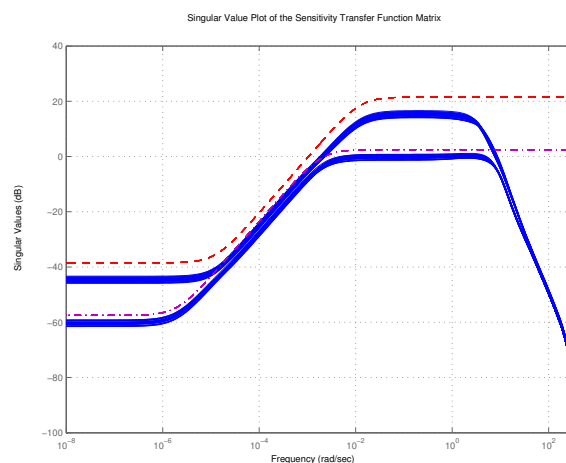


Fig. 12. Singular value plot of the sensitivity function

The frequency response plot of the singular values of disturbance transfer function matrix (output sensitivity function  $S_o$ ) is shown in Figure 12. (The inverse performance functions are shown with dashed lines.) The disturbance attenuation is more than 100 times (40 dB).



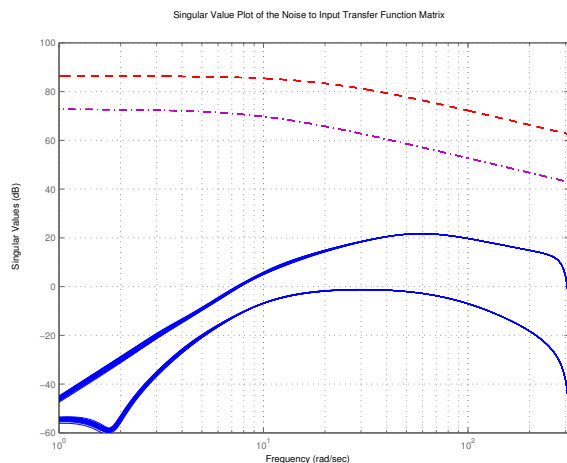


Fig. 13. Frequency response of the noise-to-control contour

The frequency response of the noise-to-control contour (Figure 13) shows that one may expect high level of the noises at the actuator inputs.

The experiments with the controller designed are done by using the laboratory set-up, shown in Figure 1 along with a PC with MATLAB<sup>®</sup>, ver. 7.1. The generation of the C driving program is done by using the Real Time Workshop, see Anon2 (2006). For this aim a Simulink<sup>®</sup> model of the closed-loop system is used with built-in driver for interface with the plant.

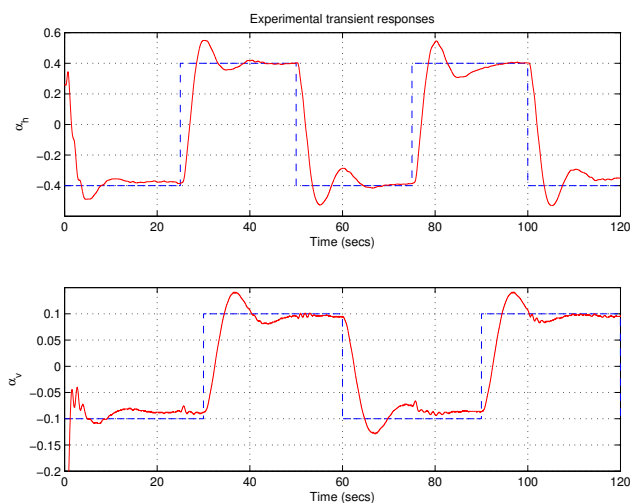


Fig. 14. Experimental transient responses

The experimentally obtained transient responses of the closed-loop system, controlled in real time with the  $\mu$ -controller designed, are shown in Figure 14. The comparison with the transient responses of the linear closed-loop system given in Figure 9 shows a good coincidence between the theoretical and experimental results.

The experimentally obtained control actions are shown in Figure 15. Due to the high level of the noises at the actuator inputs, the control actions are severely contaminated by errors.

To extract the true actuator inputs, the control signals are filtrated by using first order Butterworth filter. The

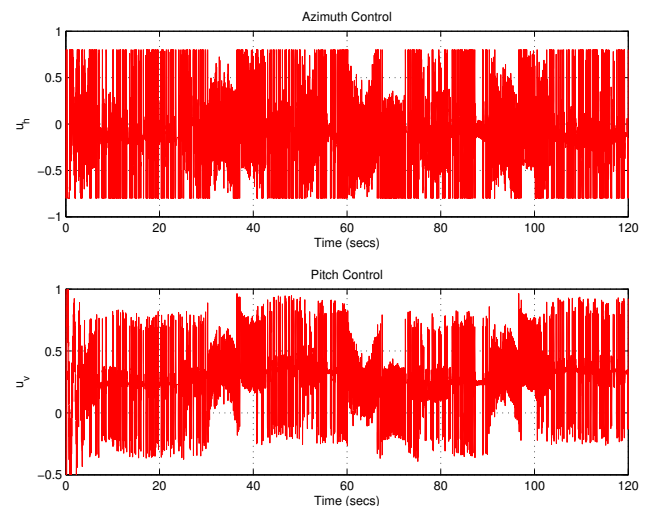


Fig. 15. Experimental control actions (noisy data)

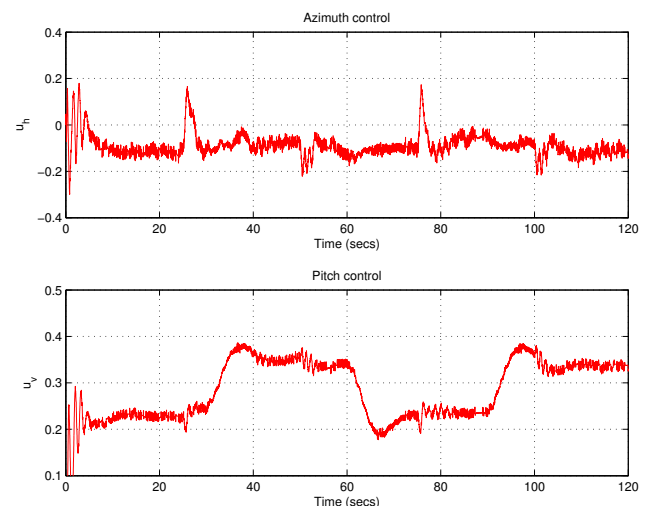


Fig. 16. Experimental control actions (after filtration)

corresponding results are shown in Figure 16 and are close to the theoretical results shown in Figure 10.

## ACKNOWLEDGEMENTS

The authors are grateful to Fadata Company whose continuous support to the Department of Systems and Control of the Technical University of Sofia made possible to perform the experiments presented in this paper.

## REFERENCES

- Anon1. *Two Rotor Aerodynamical System. User's Manual*. Inteco Ltd., 2006. <http://www.inteco.com.pl>
- Anon2. *Real-Time Workshop User's Guide*. The MathWorks, Inc., Natick, MA, 2006.
- G. Balas, R. Chiang, A. Packard, M. Safonov. *Robust Control Toolbox*. The MathWorks, Inc., Natick, MA, 2006.
- D.-W. Gu, P.Hr. Petkov, M.M. Konstantinov. *Robust Control Design with MATLAB<sup>®</sup>*. Springer, London 2005.
- K. Zhou, J. C. Doyle, K. Glover. *Robust and Optimal Control*. Prentice Hall, Upper Saddle River, NJ, 1995.